Nodeless Finite Element Method For 2d Potential Flow Problems

Wiroj Limtrakarn
Department of Mechanical Engineering, Faculty of Engineering,
Thammasat University (Rangsit Campus), Khlong Luang, Pathum Thani, 12120, Thailand.
Tel: (02) 564–3001–9 Ext. 3144, Fax: (02) 564–3010
E–Mail: limwiroj@engr.tu.ac.th

Abstract

A nodeless finite element method is presented to predict low–speed and inviscid flow behavior. The paper first describes 2D potential flow theory. Finite element formulations based on Bubnov–Galerkin method and nodeless triangular element, the computational procedure and its boundary conditions are then represented. The validated examples of the proposed technique are a rectangular plate with periodic potential function problem, flow past a circular cylinder problem and flow past an inclined ramp problem. The nodeless finite element results are compared to the solutions using linear and quadratic triangular elements to assess the efficiency of the nodeless finite element method.

Keywords: nodeless element, finite element method, potential flow

1. Introduction

Potential flow is an inviscid and incompressible flow. There are many applications that potential theory can predict the nature of flow problems such as flow in pipes, seepage flow, free surface flow, and etc. At present, there are several numerical techniques applied to predict potential flow behavior. The finite element method is one of those methods, that was employed to solve potential flow problems for many years. For 2D potential flow problems, the various element types such as linear triangular element, quadratic triangular element, quadrilateral element, and etc. are commonly used for finite element calculation.

This paper presents a nodeless finite element method for predicting the potential flow behavior. A nodeless triangular element and its element interpolation function are described. Then, the computational procedure and its boundary conditions are shown. Next, the computational nodeless finite element solutions are validated with the exact solution and finite element solutions with linear and quadratic triangular elements.

2. Theory

2.1 Governing Differential Equation

Potential flow problem is governed by Laplace's equation as shown below.

$$\frac{\partial^2 \phi}{\partial x^2} + \frac{\partial^2 \phi}{\partial y^2} = 0 \qquad (1)$$

where ϕ is the velocity potential. The relation of potential function and velocity is in the following formulation.

$$u = \frac{\partial \phi}{\partial x} \quad \text{and} \quad v = \frac{\partial \phi}{\partial y} \qquad (2)$$

2.2 Element interpolation function and finite element matrices

A nodeless triangular element consists of 3 nodes (node number 1, 2, and 3) and 3 nodeless (node number 4, 5, and 6) per element as shown in Figure 1.

Its element interpolation functions are in the form:

$$N_i(x,y) = \frac{1}{2A}\left(a_i + b_i x + c_i y\right) \quad i = 1, 3 \qquad (3)$$

$$N_4 = 4N_1 N_2 \; ; N_5 = 4N_2 N_3 \; ; N_6 = 4N_1 N_3 \qquad (4)$$

where

$$a_i = x_j y_k - x_k y_j \;, \; b_i = y_j - y_k \;, \; c_i = x_k - x_j \qquad i, j, k=1,3$$

a_i , b_i , and c_i coefficients are obtained by cyclically permuting the subscripts, and A is a triangular area.

After applying MWR in equation 1, the finite element equation based on Bubnov–Galerkin method is obtained to solve the 2D potential flow problem.

$$[K]\{\phi\} = \{Q\} \qquad (5)$$

where

$$[K] = \int_A [B]^T [B] dA$$

$$[B] = \begin{bmatrix} \frac{\partial N_1}{\partial x} & \frac{\partial N_2}{\partial x} & \frac{\partial N_3}{\partial x} & \frac{\partial N_4}{\partial x} & \frac{\partial N_5}{\partial x} & \frac{\partial N_6}{\partial x} \\ \frac{\partial N_1}{\partial y} & \frac{\partial N_2}{\partial y} & \frac{\partial N_3}{\partial y} & \frac{\partial N_4}{\partial y} & \frac{\partial N_5}{\partial y} & \frac{\partial N_6}{\partial y} \end{bmatrix}$$

$$\frac{\partial N_1}{\partial x} = \frac{y_2 - y_3}{2A} \;, \quad \frac{\partial N_1}{\partial y} = \frac{x_3 - x_2}{2A}$$

$$\frac{\partial N_2}{\partial x} = \frac{y_2 - y_1}{2A} \;, \quad \frac{\partial N_2}{\partial y} = \frac{x_1 - x_3}{2A}$$

$$\frac{\partial N_3}{\partial x} = \frac{y_1 - y_2}{2A} \;, \quad \frac{\partial N_3}{\partial y} = \frac{x_2 - x_1}{2A}$$

$$\frac{\partial N_4}{\partial x} = \frac{(y_2 - y_3)N_2 + 2(y_3 - y_1)N_1}{A}$$

$$\frac{\partial N_4}{\partial y} = \frac{(x_3 - x_2)N_2 + 2(x_1 - x_3)N_1}{A}$$

$$\frac{\partial N_5}{\partial x} = \frac{(y_3 - y_1)N_3 + 2(y_1 - y_2)N_2}{A}$$

$$\frac{\partial N_5}{\partial y} = \frac{(x_1 - x_3)N_3 + 2(x_2 - x_1)N_2}{A}$$

$$\frac{\partial N_6}{\partial x} = \frac{(y_1 - y_2)N_1 + 2(y_2 - y_3)N_3}{A}$$

$$\frac{\partial N_6}{\partial y} = \frac{(x_2 - x_1)N_1 + 2(x_3 - x_2)N_3}{A}$$

$$\{Q\} = \int_S \left(\frac{\partial \phi}{\partial x} n_x + \frac{\partial \phi}{\partial y} n_y\right)\{N\} dS$$

Pressure can be computed by using Bernoulli's equation.

$$\frac{p}{\rho} + \frac{V^2}{2} + gZ = \text{Constant} \qquad (6)$$

where V = total velocity

3. Application

In this paper, a nodeless finite element method is developed. There are three potential flow problems selected to validate the proposed method. The first problem is a rectangular plate with periodic potential function problem.. The solution is compared with the exact solution and the computational solution using a linear triangular element. The second problem is the flow past a cylinder and compared with the exact solution and is linear as well as quadratic triangular elements. The third problem is the flow past an inclined ramp problem.

3.1 Rectangular plate with periodic potential function problem

A rectangular plate with dimension 0.5x1 unit is applied with a sinusoidal potential function at the top edge. The constant zero potential function is applied along the left edge as shown in Figure 2.

This problem has an exact solution in the form:

$$\phi(x, y) = \frac{\sin(2\pi x) \times \sinh(2\pi y)}{\sinh(2\pi)} \qquad (7)$$

where $\phi_o = 1.0$ in Figure 2

After applying the nodeless finite element method, the solution of potential function distribution is shown in Figure 3.

To validate the accuracy of the nodeless finite element method, the rectangular plate is discretized in several finite element models i.e. 32 elements, 48 elements, 64 elements, 72 elements, 96 elements, 112 elements, 256 elements, and 400 elements as shown in Figure 4.

Figure 5 shows potential function solution along the x direction at y = 0.5 of the nodeless finite element solution compared with the exact solution and linear triangular element solution. Figure 6 displays the potential function solution along the y direction at x = 0.25. The results express the good accuracy of nodeless finite element method for both 32 elements and 400 elements.

The computational error has been collected in every model and displayed in Figures 7 and 8. The results show that a nodeless element has fewer errors than a linear element in every element number.

3.2 Flow past a cylinder

Flow enters from the left side of a cylinder with velocity $U_\infty = 1.0$. There is a cylinder obstructing the flow at the center as shown in Figure 9.

From the velocity boundary condition at an inlet and a wall, it can be transformed to be the potential boundary condition. Normal potential gradient at the inlet is minus the inlet velocity and zero at every wall as shown in Figure 10. The finite element model consists of 145 nodes and 242 elements.

The Nodeless finite element method is applied to compute the potential, velocity and pressure solution. The potential solution on the cylinder's wall is compared with the exact solution and computational solution using linear and quadratic triangular elements as shown in Figure 11.

The exact solution is in the form:

$$\phi = 2U_\infty \cos\theta \qquad (8)$$

Both nodeless and quadratic triangular elements give the same accuracy and their error is 1.2% less than the linear triangular element.

The nodeless finite element solution of potential and stream function are plotted in figure 12. Figure 13 shows the u–velocity and pressure distribution. The "red color" shows the maximum value and "pink color" represents the minimum value.

3.3 Flow past an inclined ramp

Flow $U_\infty = 1$ enters from the left passes an inclined ramp (45 degree) as shown in Figure 14. After flow passes an inclined ramp, it will be compressed at this corner and the pressure value is maximum at this compression corner. Then, after passing the second corner, the flow direction will realign horizontally to its initial direction. At this second corner the expansion flow happens and pressure is minimum.

The finite element model consists of 1,071 nodes and 2,000 elements as depicted in Figure 15.

After solving the problem with the nodeless finite element method, the potential distribution was obtained as shown in Figure 16, streamlines in Figure 17, u–velocity distribution in Figure 18, and pressure distribution in Figure 19, respectively.

Figure 20 shows that the potential solution obtained from nodeless and quadratic triangular elements are in good agreement.

4. Conclusions

This paper presents a nodeless finite element method to solve 2D potential flow problems. The element interpolation and finite element equations are shown. The proposed method is validated with three examples, a rectangular plate with periodic potential function, flow past a cylinder and flow past an inclined ramp. The accuracy is compared with the exact solution and finite element solution using linear and quadratic triangular elements. The results of three examples show that the accuracy of the nodeless finite element method is better than the linear element and equal to that of the quadratic triangular element methods.

5. Acknowledgements

The author is pleased to acknowledge Thammasat University for supporting this research work.

6. References

[1] Munson, B. R., *Fundamentals of Fluid Mechanics*, 4th Edition, John Wily & Sons, 2002.

[2] Streeter, V. L., *Fluid Mechanics*, McGraw-Hill Press, 1987.

[3] Zienkiewicz, O. C. and Taylor, R. L., *The Finite Element Method*, Fourth Ed., Vol. I, McGraw-Hill Press, Singapore, 2004.

[4] Akin, J. E., *Finite Element for Analysis and Design*, Academic Press, 1994.
[5] Limtrakarn, W. and Dechaumphai, P., Interaction of High-Speed Compressible Viscous Flow and Structure by Adaptive Finite Element Method, KSME International Journal, Vol. 18, No. 10, 2004.
[6] Dechaumphai, P. Finite Element Method in Engineering, Third Ed., Chulalongkorn University Press, Bangkok, Thailand, 2004.

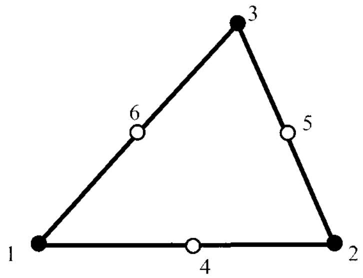

Figure 1. Nodeless element and its connectivity.

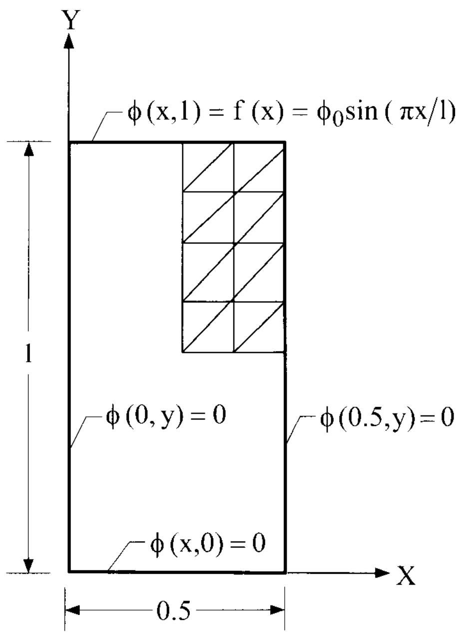

Figure 2. Problem statement of rectangular plate.

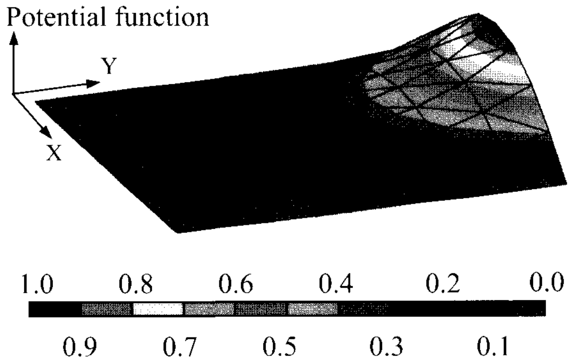

Figure 3. Potential distribution on rectangular plate.

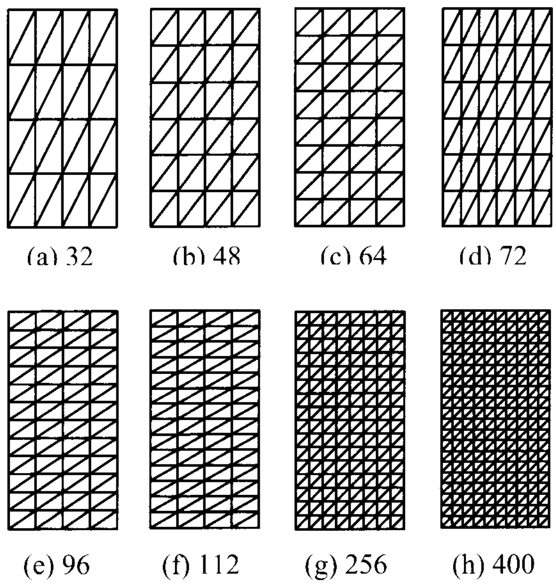

Figure 4. Finite element number of rectangular plate.

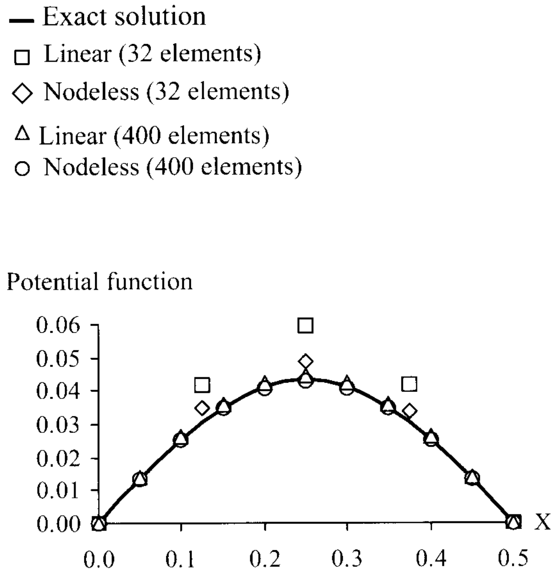

Figure 5 Potential distribution along x axis at y = 0.5.

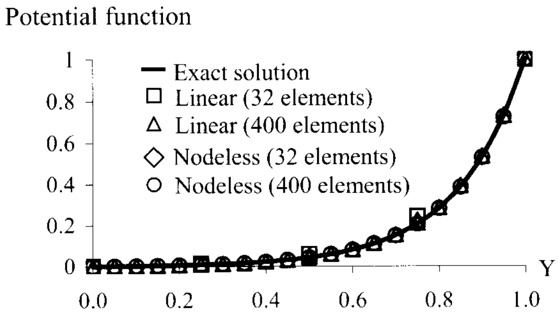

Figure 6 Potential distribution along y axis at x = 0.25

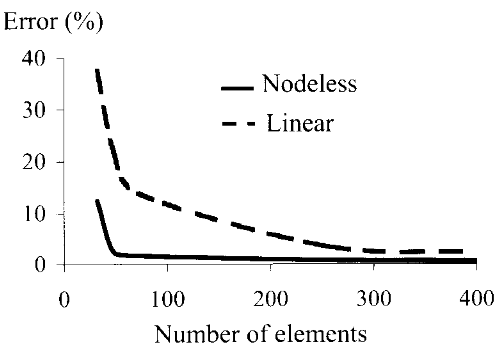

Figure 7 Error of potential function along the x axis at y = 0.5

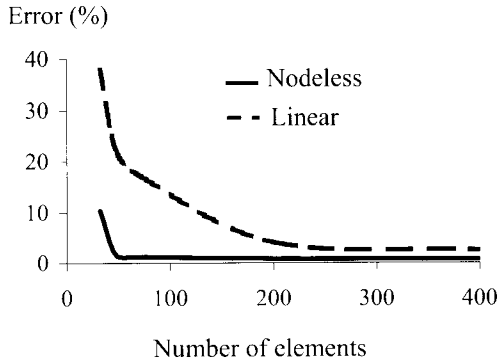

Figure 8 Error of potential function along the y axis at x = 0.25

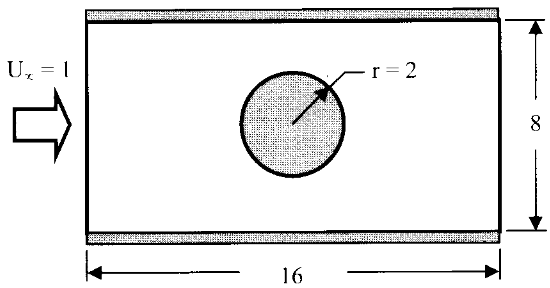

Figure 9 Flow past a cylinder problem statement.

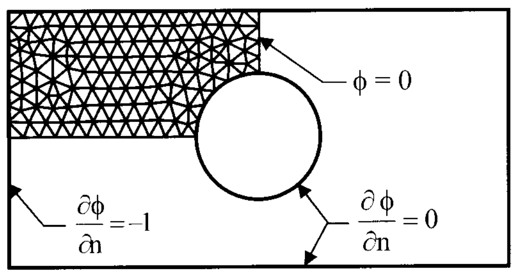

Figure 10 Finite element model and boundary conditions.

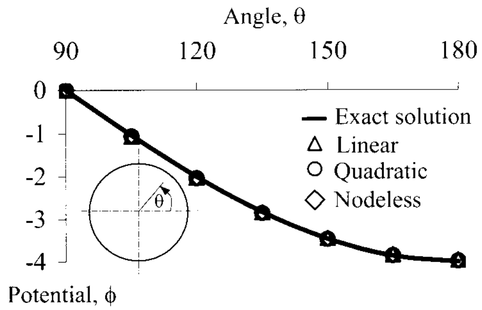

Figure 11 Plot of potential function and cylinder angle.

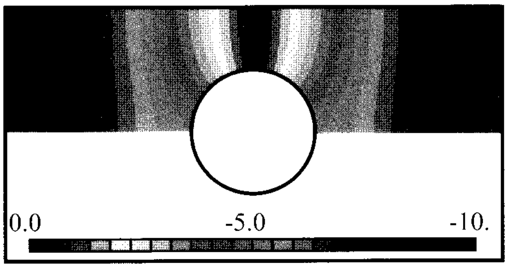

(a) Potential contours

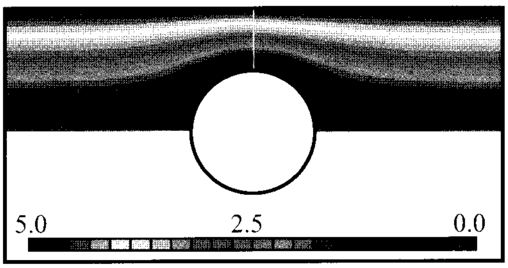

(b) Stream contours

Figure 12 Potential and stream contours.

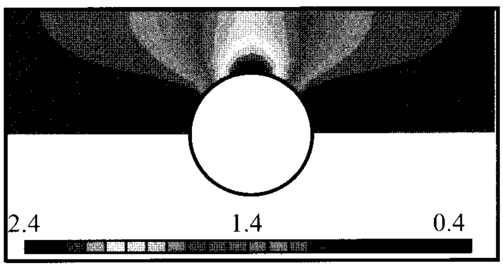

(a) u–Velocity contours

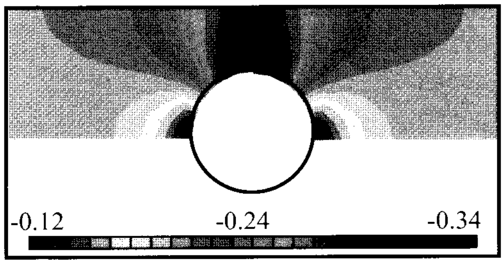

(b) Pressure contours

Figure 13 4-Velocity and pressure contours.

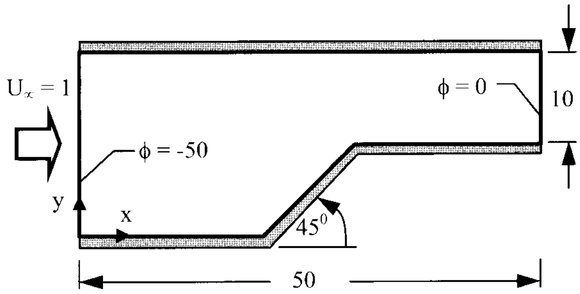

Figure 14 Flow past an inclined ramp problem statement.

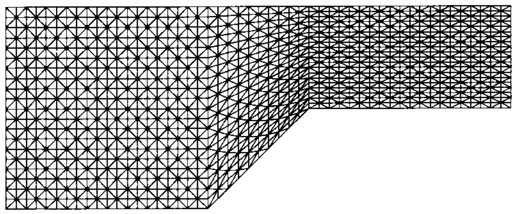

Figure 15 Finite element model.

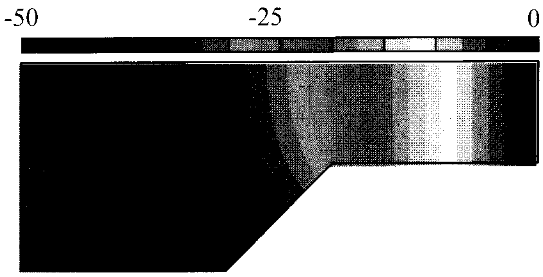

Figure 16 Potential contours of flow past an inclined ramp.

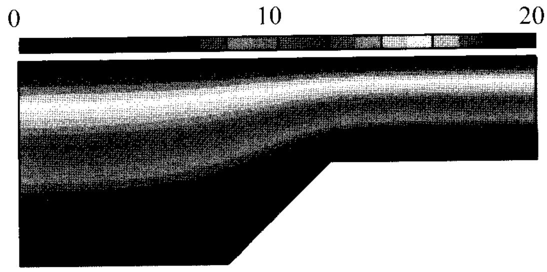

Figure 17 Streamlines of flow past an inclined ramp.

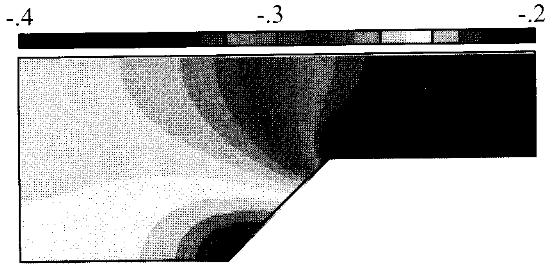

Figure 19 Pressure distribution of flow past an inclined ramp

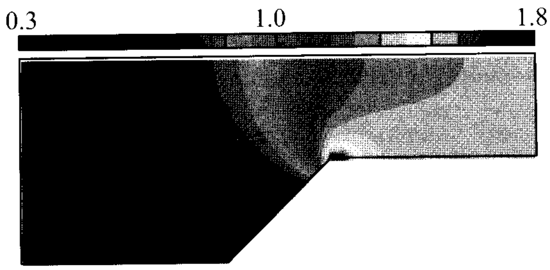

Figure 18 u – velocity distribution of flow past an inclined ramp

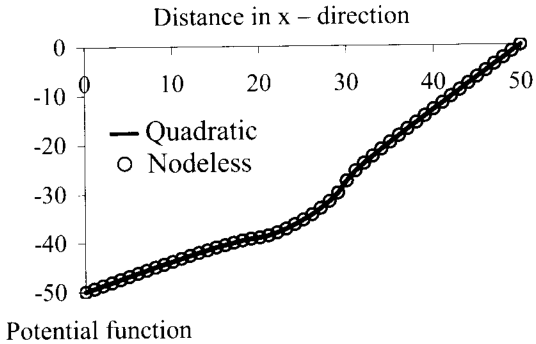

Figure 20 Plot potential function along the x – direction.